Monthly Notices
of the
ROYAL ASTRONOMICAL SOCIETY

MNRAS **439,** 3213–3224 (2014)
Advance Access publication 2014 March 1

doi:10.1093/mnras/stu048

On the number of cosmic strings

R. Consiglio,[1⋆] O. Sazhina,[2] G. Longo,[1,3] M. Sazhin[2] and F. Pezzella[4]

[1]*Dipartimento di Fisica, Università degli Studi di Napoli 'Federico II', Complesso Universitario di Monte S. Angelo ed. 6, via Cintia, I-80126 Napoli, Italy*
[2]*Sternberg Astronomical Institute, M.V. Lomonosov Moscow State University, University pr. 13, Moscow, Russia*
[3]*Department of Astronomy, California Institute of Technology, Pasadena, 90125 CA, USA*
[4]*Istituto Nazionale di Fisica Nucleare, Sezione di Napoli, Complesso Universitario di Monte S. Angelo ed. 6, via Cintia, I-80126 Napoli, Italy*

Accepted 2014 January 7. Received 2013 December 15; in original form 2013 January 31

ABSTRACT

The number of cosmic strings in the observable Universe is relevant in determining the probability of detecting such cosmic defects through their gravitational signatures. In particular, we refer to the observation of gravitational lensing events and anisotropy in the cosmic microwave background (CMB) radiation induced by cosmic strings. In this article, a simple method is adopted to obtain an approximate estimate of the number of segments of cosmic strings crossing the particle horizon that fall inside the observed part of the Universe. We show that there is an appreciable difference in the expected number of segments that differentiates cosmic strings arising in Abelian Higgs and Nambu–Goto models and that a different choice of setting for the cosmological model can lead to significant differences in the expected number of cosmic string segments. Of this number, the fraction that are realistically detectable may be considerably smaller.

Key words: cosmic background radiation – cosmology: theory – dark energy.

1 INTRODUCTION

Cosmic strings are line-like topological defects, which may have formed during a symmetry-breaking phase transition in the early Universe. The existence of topological defects in space–time was first theorized by Kibble (1976). The formation and evolution of cosmic defects were extensively studied in the subsequent decades (Vilenkin & Shellard 1995; Durrer 1999; Vachaspati 2001) for their cosmological implications. Due to the compatibility of their existence with cosmological observations and their topological stability, special interest has always been focused on cosmic strings (Shellard & Allen 1990, hereafter ASa; Hindmarsh & Kibble 1994; Hindmarsh, Stuckey & Bevis 2009). This class of linear defects is a generic prediction in quantum field theory and grand unified theories (GUTs) as well as in string and M-theories. The predicted cosmic strings are extremely thin but very massive objects, characterized by a huge energy and interactions essentially of a gravitational nature, the intensity of which is measured by the dimensionless tension parameter $G\mu/c^2$. The value of this quantity is model-dependent; for a string produced at a GUT transition it is of order 10^{-6} or 10^{-7}. Although observations rule out the idea of topological defects as an alternative theory to inflation, the coexistence of cosmological inflation and cosmic strings is apparent in those inflationary scenarios that can give rise to strings in a phase transition occurring in the last stages of inflation. This is the case of hybrid inflation models in standard cosmology as well as brane/antibrane inflation models in string cosmology, which are of hybrid inflation type. In this framework, a composite family of stable strings may exist in certain classes of models of warped compactifications or large compact extra dimensions, which yield string tensions decoupled from the *Planck* scale in the range $10^{-12} \leq G\mu/c^2 \leq 10^{-6}$ and are hence compatible with observational limits (Antoniadis et al. 1998; Arkani-Hamed, Dimopoulos & Dvali 1998; Kachru et al. 2003). Differently from solitonic strings, cosmic superstrings can exist as F and D strings, leading to more complicated F–D networks involving the formation of junctions between strings of different tensions (Jones, Stoica & Henry Tye 2003; Copeland, Myers & Polchinski 2004). Although they can have different properties related to the different contexts in which they arise, cosmic superstrings are expected to share with ordinary solitonic strings the same scale-invariance property of the characteristic length-scales of the network they can form.

Since their energy density may influence the dynamics of the Universe, consistency with present day observations imposes constraints on the number density of cosmic strings. To date, cosmic (super)strings are still theoretical objects; nevertheless, theoretical advances together with upcoming observational data might provide stronger constraints on their characteristic parameters and make their eventual detection a test of the generic predictions of standard or alternative theories. Observations of such strings would provide direct information on the fundamental physics and evolution of our Universe and maybe the first experimental evidence of a string theory cosmological model underlying the structure of space–time.

Of the two components of an evolving string network, subhorizon closed loops and long strings (i.e. infinite strings and large

⋆E-mail: rosa.consiglio@na.infn.it

© 2014 The Authors
Published by Oxford University Press on behalf of the Royal Astronomical Society

Downloaded from http://mnras.oxfordjournals.org/ at California Institute of Technology on May 29, 2014

loops with a curvature radius much larger than the horizon size), we are concerned in particular with the long string component, owing to the effects produced by the presence of this component of the network. Cosmic (super)strings may have a number of cosmological effects. The most interesting observational signatures stem from their gravitational interactions. While specific signatures are expected in models where strings couple to other forces, gravitational effects are common to all cosmic (super)strings and are controlled by the dimensionless tension parameter. A special class of gravitational effects originates from the string's peculiar way of deforming the space–time around it. The space–time around a cosmic string is conical; namely, it is flat everywhere except for a missing wedge where points on the opposite edges are identified. Thus, space–time looks like a cone with a singularity located at the apex of the cone. Any circular path at a constant distance from the apex around the string is less than a circumference by the deficit angle $\Delta = 8\pi G\mu/c^2$. This geometry leads to observable effects, such as the Kaiser–Stebbins effect (KS: Kaiser & Stebbins 1984) and gravitational lensing. The former appears as line discontinuities in the cosmic microwave background (CMB) temperature caused by a segment of cosmic string moving between the observer and the cosmological photosphere as photons passing by the string move perpendicularly to the plane that contains the string segment. Photons from the last scattering surface streaming by either side of the string will be observed with a redshift or blueshift (ahead of or behind the moving string respectively) proportional to the string tension and the string velocity transverse to the line of sight. Gravitational lensing by a long cosmic string occurs as light from a distant source beyond the string may reach the observer along two different paths, around either side of the string, thus producing a double image of the source with angular separation proportional to the conical deficit angle $8\pi G\mu/c^2$.

The observational signatures of cosmic strings depend on their characteristic parameters, such as string tension and velocity, and on the details of the evolution of the string network, which in turn depends on what happens when two strings intersect. A fundamental feature that differentiates a network of cosmic superstrings from a network of ordinary field-theory cosmic strings is their reduced intercommutation probability P, which determines the evolution of a string network towards a scaling regime. For classical cosmic strings, the string tension is directly related to the energy scale of the symmetry breaking and the intercommutation probability is essentially $P = 1$. In fact, even though ultrarelativistic Abelian Higgs strings can pass through each other due to a double intercommutation, with the net result that no ends are exchanged (Achucarro & de Putter 2006), the typical velocities found in simulations for scaling networks of cosmic strings are below the ultrarelativistic threshold, so that the assumption $P = 1$ generally holds. For F–D networks, P can be significantly less than unity, depending on the type of string and compactification and on the string coupling constant g_s. As a consequence of the smaller intercommutation probabilities associated with strings of different tensions, in a cosmic superstrings network each type of string may have a different number density. This means that the same fraction of CMB anisotropy can be sourced by either many light strings or a few heavy ones, but it also means that the total number of strings in the network must be increased by some factor related to the intercommutation probabilities, which implies stronger constraints on tensions. The eventual presence of Y-shaped junctions of two strings joined by a third after intercommutation processes could be detected by cosmic string gravitational lensing or by observation of the KS effect. In the latter case, we expect to observe a different temperature in each of the three patches of sky, while in the former case the relativistic motion of the binding strings could also lead to an enhancement of the cosmic string lensing angle by some factor, which would be moderate for a typical network motion (Avgoustidis & Shellard 2005; Henry Tye, Wasserman & Wyman 2005; Jackson, Jones & Polchinski 2005; Pourtsidou et al. 2011).

On the other hand, the root-mean-square (rms) velocities comparable to the speed of light found in numerical simulations (Bennett & Bouchet 1990, BB hereafter; Allen & Shellard 1990, ASb hereafter; Martins & Shellard 2006, MS hereafter; Ringeval, Sakellariadou & Bouchet 2007, RSB hereafter; Bevis et al. 2007; Battye & Moss 2010, BM hereafter; Blanco-Pillado, Olum & Shlaer 2011, BPOS hereafter) could be sufficiently high to guarantee the detectability of their signatures in the CMB radiation, at least under certain ideal conditions, if such strings do exist and are field theoretical cosmic strings. As for cosmic superstrings, although the rms velocities can be close to the flat space–time value $c/\sqrt{2}$, the tension parameter associated with the F component, for a string coupling constant of order 10^{-2}, is smaller than that of the other components, which have values very close to those of ordinary cosmic strings. Such small values of tensions are still unexplored by means of current technology.

The number of cosmic (super)strings contained in the volume of the effective observable Universe is also a relevant parameter to determine the probability of observing cosmic strings in gravitational lensing events as well as the density of step-like temperature discontinuities related to the KS effect (Sazhina et al. 2008; Sazhin et al. 2010). More precisely, the significant parameter is the number of string segments that can be considered approximately straight in a network of random walk cosmic (super)strings, since these are expected to have a greater probability to leave detectable and unambiguous signals in the observed volume of the Universe. In the present article, we consider both cases: field theory cosmic strings and string theory cosmic superstrings, comparing and discussing the results.

In Section 2 we describe a simple method to obtain an approximate estimate of the number of segments of cosmic strings crossing the observable Universe. In particular, for observational relevance, we consider the volume inside the last scattering surface and inside the sphere of optical sources, respectively, for the KS effect and gravitational lensing observations. The discourse is broadened to string networks embedded in cosmological backgrounds, variants of ΛCDM, where the constant parameter Λ is replaced with a dynamical scalar field. For comparison of results we consider, for simplicity, spatially flat cosmological models where the cosmic fluid is a mixture of matter and quintessence or a phantom constituent (a time-varying component of the energy density of the Universe with negative or supernegative pressure, $p < -\rho$) characterized respectively by the ratio of pressure to energy density in the ranges $-1 \leq w < 0$ and $w < -1$, whereas $w = -1$ coincides with the cosmological constant case. In the above intervals we choose in particular $-1 \leq w_{\rm Q} \leq -0.5$ and $w_{\rm P} = -1.5$ for the quintessence (Q) and phantom (P) components, as they are compatible with constraints from large-scale structure and CMB observations combined with SNe Ia data. In Section 3, we extend the approach of the previous section to address the case of cosmic superstrings. In Section 4, some features connected with numerical simulations and their underlying models are outlined in relation to the scaling property of the string network, upon which the estimate of the number of string segments relies. Finally, we discuss our results with particular reference to the range of redshifts in the visible Universe, where the calculation of the number of string segments can be trusted,

Downloaded from http://mnras.oxfordjournals.org/ at California Institute of Technology on May 29, 2014

taking into account the information about scaling regimes provided by numerical simulations.

Without a loss of generality, in what follows we shall use the cosmological parameters of the ΛCDM concordance model, which fit the majority of observations (information on the cosmological parameters obtained from the site http://lambda.gsfc.nasa.gov/product/map/dr5/parameters.cfm):

$$\Omega_{\rm m} \simeq 0.27, \qquad \Omega_\Lambda \simeq 0.73, \qquad H_0 \simeq 71\,{\rm km\,s^{-1}\,Mpc^{-1}}. \tag{1}$$

2 NUMBER OF COSMIC STRING SEGMENTS CROSSING THE OBSERVABLE UNIVERSE

2.1 Cosmic string networks in a ΛCDM Universe

An approximate estimate of the number of string segments crossing a given volume of the observable Universe can be obtained, taking into account that Kibble's one-scale model can conveniently be used to study large-scale properties. The single scale L, which can be identified with the persistence length or the mean interstring distance, is defined as the length such that any volume L^3 will contain, on average, a string segment of length L. By causality, L is bounded by the size of the particle horizon, $d_{\rm PH}$:

$$L(t) = A_i\, d_{\rm PH}(t), \tag{2}$$

where

$$0 < A_i \leq 1, \qquad i = {\rm r, m}, \tag{3}$$

with r ≡ radiation and m ≡ matter. The quantity

$$A_i^{-1} = \frac{d_{\rm PH}}{L} \tag{4}$$

expresses the scaling property: in the radiation-dominated era (after the transient friction-dominated period) and matter-dominated era (after the radiation–matter transitional period), the network approaches a scaling regime in which L remains a constant fraction of the particle horizon, as well as the energy in the form of strings remaining a constant fraction of the total energy of the Universe. Therefore, the above quantity is the result of the efficiency of the various energy-loss processes that a network of strings undergoes. This provides us with an elementary cell, containing a single string segment, the volume of which can be calculated since A_i is known from numerical simulations, and the (physical) particle horizon distance $d_{\rm PH}$:

$$d_{\rm PH}(z_*) = \frac{c}{H_0}\frac{1}{1+z_*}\int_{z_*}^{\infty}\frac{{\rm d}z}{E(z)}, \tag{5}$$

where

$$E(z) = \left[\sum_{i\in I}\Omega_i(1+z)^{3(w_i+1)}\right]^{1/2}, \qquad I = \{\Lambda, k, {\rm m}, {\rm r}\}, \tag{6}$$

with w_i the equation-of-state parameter for the ith fluid. Considering the entire volume of the observable Universe – defined by the distance to the particle horizon – circumscribed by a cube having side $2d_{\rm PH}(z)$ (5), the total number of string segments for all z in the radiation- and matter-dominated eras,

$$N^{\rm r,m}(z) = \frac{[2\,d_{\rm PH}(z)]^3}{L^3(z)} = \frac{8}{A^3_{\rm r,m}}, \tag{7}$$

remains constant in each of the two cosmological eras of the Universe. Now, suppose we consider only a fraction of the volume of the observable Universe observed at time t_*. Defining the distance travelled by a photon emitted at time $t < t_*$,

$$d(z_*, z) = \frac{c}{H_0}\frac{1}{1+z_*}\int_{z_*}^{z}\frac{{\rm d}z'}{E(z')}, \tag{8}$$

where

$$d(z_*, z) = B(z_*, z) d_{\rm PH}(z_*), \tag{9}$$

with

$$0 < B(z_*, z) \leq 1, \tag{10}$$

the fraction of the total number of string segments that falls inside the volume $[2d(z_*, z)]^3$ can be computed as

$$N^{\rm r,m}(z_*, z) = \frac{[2\,d(z_*, z)]^3}{L^3} = \frac{8\,B^3(z_*, z)}{A^3_{\rm r,m}}. \tag{11}$$

$B(z_*, z) = 1$ gives the total number of string segments in the particle horizon volume (7) for each cosmological epoch.

The particle horizon delimits the part of the Universe beyond which no causal connection exists. However, an observer cannot even see that far, the view of the Universe at any time being limited to the largest volume visible in light. Information on matter, as well as cosmic strings lying between such a visual horizon and the particle horizon, could only be obtained through the gravitational radiation they emit, which cannot as yet be detected directly. Therefore, in particular, we are concerned with the volume contained inside the spherical surface named the *last scattering surface* (LSS), given by the set of points in space at a distance such that photons emitted at decoupling time reach present-day observers. Then, at any time $t \geq t_{\rm LSS}$, belonging to the matter-dominated era, the distance to any point inside the LSS can be written as the distance travelled by a photon from the emission point at a time $t \geq t_{\rm LSS}$ to an observer at the present time t_0:

$$d(z) = \frac{c}{H_0}\int_0^z \frac{{\rm d}z'}{\sqrt{\Omega_{\rm m}\,(1+z')^3 + \Omega_\Lambda}}. \tag{12}$$

Equation (12) defines the effective observable Universe, i.e. our backward light cone. Let us now consider a cube with side equal to the diameter of the spherical volume centred on the present-time observer, $2d(z)$, with

$$z_0 < z \leq z_{\rm LSS}, \tag{13}$$

where $z_0 = 0$ is the redshift at the present time and $z_{\rm LSS} = 1100$ is the redshift corresponding to the last scattering time. The largest cube, for $z = z_{\rm LSS}$, circumscribes the CMB sphere so that all strings that enter the last scattering surface and may have potentially observable effects on the CMB radiation are inside this volume. For any given value of redshift in the interval (13), the number of string segments crossing the corresponding volumes is the fraction of (7) given by

$$N(z) = \frac{8B^3(z)}{A^3_{\rm m}}, \tag{14}$$

shown in Table 1 for different Nambu–Goto (NG) and Abelian Higgs (AH) simulations.

2.2 Dark energy cosmological models

In the previous section, we chose for definiteness a particular Friedmann–Robertson–Walker (FRW) cosmology, the ΛCDM model, as the cosmological background for the evolving strings network. In the present section, we generalize to a broader class

Downloaded from http://mnras.oxfordjournals.org/ at California Institute of Technology on May 29, 2014

Table 1. Cosmic string parameters (where v_r and v_m are respectively the rms velocities in the radiation- and matter-dominated eras) from high-resolution simulations performed from the 1990s to date. The results obtained by Battye–Moss (BM) refer to Unconnected Segment Model (USM) modelling of Nambu–Goto (NG) and Abelian Higgs (AH) strings. All other results, save those obtained by Bevis and coauthors (Bevis et al. 2010, hereafter BHKU), refer to NG simulations.

Model par	BB	ASa,ASb	MS	RSB	BHKU (AH)	BM (NG/AH)	BPOS	Δz
$\frac{G\mu}{c^2}$	4×10^{-6}	1.5×10^{-6}		7×10^{-7}	1.8×10^{-6}	$(2.6/6.4) \times 10^{-7}$		
v_r	$0.66c$	$0.62c$	$0.63c$		$0.5c$	$0.65c/0.4c$	$0.63c$	
v_m	$0.61c$	$0.58c$	$0.57c$		$0.5c$	$0.60c/0.4c$	$0.59c$	
A_r	0.14	0.13	0.13	0.16	0.26	0.13/0.35	0.15	
A_m	0.18	0.17	0.20	0.19	0.29	0.21/0.35	0.17	
$N(z)$	5–300	6–360	4–220	4–260	1–73	3–190/1–40	6–360	(0.5, 7]
$N(z)$	340–960	400–1100	250–700	290–820	80–230	210–610/46–130	400–1100	[8, 100]
$N(z)$	(1200, 2600)	(1500, 3300)	(900, 3300)	(1100, 1800)	(300, 410)	(780, 3300)/170	(1500, 2100)	1100

of models by replacing the static homogeneous energy component, with positive energy density and negative pressure Λ, with a dynamical, time-dependent and spatially inhomogeneous energy component, named *dark energy*, the negative pressure of which drives the accelerated expansion of the Universe currently observed. In particular, the class of cosmological models we consider comprises spatially flat FRW space–times dominated by dark energy at late times, after radiation (photons and relativistic neutrinos) and matter (ordinary and cold dark matter) dominance.

The space–time, for a spatially flat expanding universe, is described by the metric

$$\mathrm{d}s^2 = c^2\mathrm{d}t^2 - a^2(t)\mathrm{d}\boldsymbol{x}^2. \tag{15}$$

Defining the conformal time η by

$$\mathrm{d}\eta = \frac{c\mathrm{d}t}{a(t)}, \tag{16}$$

the metric can be conveniently expressed in terms of η as

$$\mathrm{d}s^2 = a^2(\eta)\left(\mathrm{d}\eta^2 - \mathrm{d}\boldsymbol{x}^2\right). \tag{17}$$

The scalefactor $a(\eta)$ is determined from the Friedmann equation, which can be written in the form

$$\left(\frac{\mathrm{d}a(\eta)}{a^2(\eta)\mathrm{d}\eta}\right)^2 = H_0^2\left[\Omega_m\left(\frac{1}{a(\eta)}\right)^3 + \Omega_{DE}\left(\frac{1}{a(\eta)}\right)^{3(1+w)}\right], \tag{18}$$

where Ω_{DE} is the dark energy density parameter, related to the current contribution of about 73 per cent to the total energy density of the Universe, the budget for which should also contain the contribution of radiation (as well as spatial curvature), which we have neglected as it is about one per cent. $w = w_Q$, w_P is the ratio of pressure to energy density that defines the equation of state for dark energy:

$$p_{DE} = wc^2\rho_{DE}. \tag{19}$$

Current cosmological observations restrict the values of the equation-of-state parameter to the interval

$$w \in [-1.5, -0.5]. \tag{20}$$

Scalar field models can yield a time-varying equation-of-state parameter, such that at large redshifts w corresponds to quintessence ($w > -1$) while in later stages, at low redshifts, w becomes much more negative, denoting a phantom energy component ($w < -1$). In the very late Universe, the phantom energy density ($\rho_P > 0$) can grow, allowing the parameter w to reach an observationally compatible value slightly below -1 (Caldwell 2002; Copeland, Sami & Tsujikawa 2006; Frieman, Turner & Huterer 2008).

Using the conformal gauge, photons travelling on radial null geodesics, given by $\mathrm{d}s^2 = 0$, move a unit comoving distance per unit conformal time, $\mathrm{d}\eta = \pm\mathrm{d}x$. Thus, in the conformally flat metric the light cones are Minkowskian and the speed of light is 1. Hence, in conformal coordinates, light emitted at conformal time η_e will be observed at conformal time η_o at comoving distance:

$$D(z_o, z_e) = \eta_o - \eta_e. \tag{21}$$

The distance to the emitting source at redshift z_e can then be obtained from the first Friedmann equation as

$$D(z_o, z_e) = \frac{c}{H_0}\int_{z_o}^{z_e} \frac{\mathrm{d}z}{(1+z)^{3/2}\sqrt{\Omega_m + \Omega_{DE}(1+z)^{3w}}}. \tag{22}$$

In this context, the expression for the characteristic length-scale of the network is $L_{DE}(t) = A_{m,DE}D_{PH}(t)$, where the distance to the particle horizon in terms of z is

$$D_{PH}(z_o) = \frac{c}{H_0}\int_{z_o}^{\infty} \frac{\mathrm{d}z}{(1+z)^{3/2}\sqrt{\Omega_m + \Omega_{DE}(1+z)^{3w}}}, \tag{23}$$

with $z_o \equiv z_0 = 0$ for a present-time observer. Using the proper total length in long strings in a particle horizon volume, we can define a quantity that is constant as long as the scaling law holds:

$$\rho_{LS}\frac{d_{PH}^2}{\mu} = \frac{1}{A_{r,m}^2}. \tag{24}$$

The long string contribution to the total energy density ρ of the Universe scales like radiation in the radiation-dominated era and like matter in the matter-dominated era. Choosing $\Omega_X = 0.73$, for $X = \Lambda$, Q, P, ρ_{LS} does not change with the cosmological setting, since it is assumed to be a constant fraction of the same ρ. Thus, for quintessence and phantom field models we have

$$A_{r,m,DE} = \left(\frac{d_{PH,\Lambda}(z)}{d_{PH,DE}(z)}\right)^{3/2} A_{r,m,\Lambda}, \qquad DE = Q, P, \tag{25}$$

such that

$$\rho_{LS} = \frac{\mu}{L_X^2}, \qquad X = \Lambda, Q, P \tag{26}$$

remains the same for each model.

Since the string length density per unit volume L^3, $1/L^2$, is the same for each of cosmological models considered, the number of string segments changes, as we show in Fig. 1 and Table 2. The values of $A_{m,Q}$ and $A_{m,P}$ have been derived from the mean values of $A_{m,\Lambda}$ related to the NG and AH simulations of Table 1.

Downloaded from http://mnras.oxfordjournals.org/ at California Institute of Technology on May 29, 2014

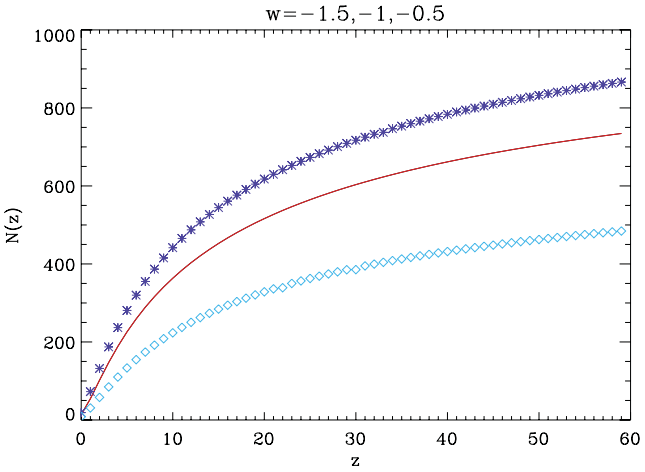

Figure 1. $N(z)$ plotted for the equation-of-state parameter varying inside the interval $w \in [-1.5, -0.5]$, for the NG parameters $A_{\mathrm{m},X}$, $X = \mathrm{P}, \Lambda, \mathrm{Q}$. The solid curve corresponds to $w = -1$, stars correspond to $w = -1.5$ and diamonds correspond to $w = -0.5$.

3 COSMIC SUPERSTRINGS

Cosmic superstrings can form at the end of inflation in brane inflationary scenarios in string theory. They can exist with small tensions, in configurations that are stable over cosmological time-scales and can stretch over cosmological distances as well as solitonic strings. As previously mentioned, a network of cosmic superstrings can in principle be distinguished from a network of field theory cosmic strings by the possibility of forming trilinear vertices connected by a segment of string when strings of two different types cross and by the reduced intercommutation probability. The strength of the interaction between the colliding strings depends on the string coupling constant g_{s}, the scale of the confining potential (the values of which are not known), the details of compactification, the relative velocity of the strings and their intersection angle. For the class of models based on large or warped compact extra dimensions, the reconnection probability for D strings is found to be in the range $0.1 \lesssim P \lesssim 1$, whereas that for F strings is $10^{-3} \lesssim P \lesssim 1$. When collisions involve strings of different type, the reconnection probability can vary from 0 to 1.

New energy-loss mechanisms are also available. As with solitonic strings, oscillating string loops can lose energy through gravitational radiation. In addition, for cosmic superstrings, massless and massive moduli fields, including the dilaton, are also expected to be radiated away. Power radiation by D-string loops also includes massless Ramond–Ramond (R–R) fields. Since the zero modes of the graviton and R–R fields belong to the massless sector of the closed string spectrum, depending on the underlying string theory inflationary model, these two channels for energy loss might be comparable with each other (Firouzjahi 2008).

Analytical and numerical studies show the following results. First, although complicated networks may form initially, a scaling regime is eventually reached in which the characteristic lengths are a constant but different fraction of the particle horizon. Second, in a scaling superstring network the three lightest strings, (1, 0), (0, 1) and (1, 1) (respectively F and D strings and the lightest FD bound state) dominate the string number density, whatever the value of g_{s}.

For a large value of the string coupling, $g_{\mathrm{s}} \sim \mathcal{O}(1)$, most of the network energy density is in the lightest (1, 0) and (0, 1), the tensions of which in this case are approximately equal, being $\mu_{\mathrm{D}} = \mu_{\mathrm{F}}/g_{\mathrm{s}}$. At smaller values of $g_{\mathrm{s}} \sim \mathcal{O}(10^{-2})$, the (1, 0) component becomes much lighter than both the (0, 1) and (1, 1) strings and dominates the string number density although, because of their much larger tension, the energy density of the network can be dominated by the less numerous components (0, 1) and (1, 1).

The D strings, being much heavier than the F strings, may evolve independently of the F strings and reach the scaling regime like a single D-strings network. After the D strings settle down the scaling distribution on a given length-scale, the F strings in turn may evolve like a single F-string network.

Allowing for specific details that depend on the model-dependent value of the effective volume of the compact dimensions, in each of the two scaling behaviours at large or small values of g_{s} the energy density of the multitension network appears to be dominated by nearly single-tension strings.

However, these two distinct scaling behaviours predicted for a network of cosmic superstrings in principle can be seen in the power spectra of the CMB anisotropies they source, which depend on the type of strings involved. At different values of g_{s}, strings with different correlation lengths can dominate the spectra and determine the position of the main peak. In the one-scale model, the characteristic length-scale $L(t)$ of the network represents both the correlation length in directions along the string and the average inter-strings distance, supposed to be approximately equal. Thus, string networks with higher (lower) number density have smaller (larger) correlation lengths. The values of the correlation length and the rms velocity (both dependent on g_{s}) determine the shapes of the string-induced CMB spectra.

The extension of the velocity-dependent one-scale model to a multitension F–D network requires defining a specific length-scale for any type of string $L_i(t) = A_{r/m,i}\, d_{\mathrm{PH}}(t)$ ($i = \mathrm{F}, \mathrm{D}, \mathrm{FD}$) and the energy density for any component of the network $\rho_i = \mu_i / L_i^2$.

The tension of each component in flat space–time is given by

$$\mu_i \equiv \mu_{(p_i,q_i)} = \frac{\mu_{\mathrm{F}}}{g_{\mathrm{s}}} \sqrt{p_i^2 g_{\mathrm{s}}^2 + q_i^2}, \tag{27}$$

Table 2. The approximate number of string segments for different values of the equation-of-state parameter.

Model	P (NG)	P (AH)	Λ (NG)	Λ (AH)	Q (NG)	Q (AH)
w	–1.5	–1.5	–1	–1	–0.5	–0.5
A_{m}	0.18	0.30	0.19	0.32	0.22	0.36
A_{r}	0.17	0.29	0.18	0.31	0.20	0.35
$N(z)$ $z \in (0.5, 7]$	6–320	1–70	4–260	1–54	2–140	1–33
$N(z)$ $z \in [8, 100]$	360–980	78–210	290–820	61–170	160–510	37–120
$N(z)$ $z = 1100$	(1200–1500)	(270–300)	(1100–1200)	(220–240)	(670–900)	(150–170)

Downloaded from http://mnras.oxfordjournals.org/ at California Institute of Technology on May 29, 2014

Table 3. Expected number of string segments of the various components of an F–D network in the small g_s regime for two ranges of redshift, $z \in (0.6, 7]$ and $z \in [8, 100]$, and at the last scattering epoch.

	$W = 1 \quad g_s = 0.04$	
$0.6 \lesssim z \lesssim 7$	$8 \lesssim z \lesssim 100$	$z = 1100$
$4000 \lesssim N_F(z) \lesssim 2.6 \times 10^5$	$2.9 \times 10^5 \lesssim N_F(z) \lesssim 8.2 \times 10^5$	$1.1 \times 10^6 \lesssim N_F(z) \lesssim 1.8 \times 10^6$
$2 \lesssim N_D(z) \lesssim 66$	$73 \lesssim N_D(z) \lesssim 210$	$270 \lesssim N_D(z) \lesssim 330$
$1 \lesssim N_{FD}(z) \lesssim 35$	$40 \lesssim N_{FD}(z) \lesssim 110$	$140 \lesssim N_{FD}(z) \lesssim 170$

Table 4. Expected number of string segments of the various components of an F–D network in the large g_s regime, for $z \in (0.6, 7]$ and $z \in [8, 100]$ and at the last scattering epoch.

	$W = 1 \quad g_s = 0.9$	
$0.6 \lesssim z \lesssim 7$	$8 \lesssim z \lesssim 100$	$z = 1100$
$21 \lesssim N_F(z) \lesssim 1300$	$1500 \lesssim N_F(z) \lesssim 4200$	$5400 \lesssim N_F(z) \lesssim 9300$
$5 \lesssim N_D(z) \lesssim 300$	$340 \lesssim N_D(z) \lesssim 960$	$1200 \lesssim N_D(z) \lesssim 1800$
$0 \lesssim N_{FD}(z) \lesssim 4$	$5 \lesssim N_{FD}(z) \lesssim 14$	$18 \lesssim N_{FD}(z) \lesssim 20$

where $\mu_F = \mu_{(1,0)}$ and $\mu_D = \mu_{(0,1)}$ are respectively the tensions of the lightest F string carrying charge (1, 0) and D string carrying charge (0, 1); μ_{FD} becomes essentially $\mu_{(1,1)} = (\mu_F/g_s)\sqrt{g_s^2 + 1}$, as the lightest bound state only appears to dominate the string number density.

Following the results obtained in Pourtsidou et al. (2011, see therein for more details on the model), in the two limiting values of the coupling $g_s = 0.04$ and $g_s = 0.9$ and for a particular value of the volume factor associated with compactification $W = 1$, corresponding to a compactification close to the string scale, we find for each component of the network the results represented in Tables 3 and 4 for the string number in the various ranges of redshift that are observationally interesting.

In both g_s regimes, the F component of the network gives a large contribution to the total number of string segments in a volume corresponding to a given z:

$$N(z) = \sum_{i=1}^{3} N_i(z). \tag{28}$$

The results represented in Table 3 show that for $g_s = 0.04$ the expected number of string segments for the F component appears to be exceedingly large. In fact, at small redshifts, down to $z = 0.6$, the order of magnitude of $N(z)$ is 10^3 against a value of about 20 obtained for $g_s = 0.9$. This, on the one hand, suggests we should look at an intermediate regime to find results that are hopefully realistic. On the other hand, the tension parameter associated with the F component for $g_s = 0.04$ is smaller than that of the other components, which have values very close to those of ordinary cosmic strings. Such small ranges of tensions are still unexplored by means of current technology. In fact, the CMB spectra sourced by a F–D network, normalized to give that cosmic strings cannot contribute more than 10 per cent of the total CMB temperature anisotropy, correspond to the following values of the tension parameter:

$$\frac{G\mu_F}{c^2} = 1.8 \times 10^{-8}, \qquad \frac{G\mu_F}{c^2} = 2.1 \times 10^{-7}, \tag{29}$$

respectively for $g_s = 0.04$ and $g_s = 0.9$.

Despite the higher values of the rms velocities that the F component may reach in the radiation era $v_{r,F} \sim 0.7c$, with very small decrease in the matter era in the small g_s regime, for $W = 1$ a tension parameter of order 10^{-8} results in a value of amplitude of the temperature anisotropy of order 10^{-7}, which is still out of reach, being the order of magnitude of the *Planck* resolution at temperature 10^{-6}.

In the large g_s regime, the rms velocity of the F component is smaller ($v_{r,F} \sim 0.67c$), with more evident decrease in the matter era, but the tension parameter (29) is of the same order of magnitude as field theory cosmic strings. The length-scale parameter is also comparable to that of ordinary cosmic strings.

The one-scale model is unable to provide a proper description of the network properties at scales close to the string width, which is set by the scale of the symmetry-breaking phase transition in field theory and by the fundamental string scale, warp factors associated with the space–time curvature and the size of the internal six-dimensional manifold in string theory. On the other hand, this model describes well not only the large-scale features of the scaling network but also the deviation from scaling.

4 DISCUSSION AND RESULTS

4.1 General framework

The number of string segments $N(z)$ has been determined in the range of redshifts of interest for observations using the constant quantity A_m associated with the scaling law, thus assuming that the network has already reached the scaling regime in the matter-dominated era by the last scattering time, which is the upper limit of the range of redshifts (13). As a matter of fact, there is a transition period between the radiation-dominated and matter-dominated eras, where the string network will be far from the type of equilibrium that characterizes a scaling solution for a time, dependent on how fast the network's response to the change in expansion rate is. Thus, the range of redshifts, in the matter-dominated era, within which we can trust a string segment distribution based on the scaling property could be well below z_{LSS} and hence below the range of radio surveys searching for cosmic string signatures in the CMB radiation. A similar limit, this time at very small redshifts, namely $z \approx 0.5$, also needs to be taken into account, since there is a further transition between the matter-dominated era and the dark-energy-dominated era (Riess et al. 2004; Bolotin, Lemets & Yerokhin 2012). The effect of this transition to a cosmological era where the Universe expands exponentially will be a reduction of the string velocity, which prevents reconnection, affecting the scaling behaviour and, at the same time, a dilution that might lead to a small number density of the leftover network (Albrecht, Battye & Robinson 1998; Battye, Robinson & Albrecht 1998).

The scaling property that implies it makes sense to consider the possibility of the existence of strings in our Universe and search for their observable effects is the first fundamental information about a network of cosmic strings yielded by numerical simulations. For

Downloaded from http://mnras.oxfordjournals.org/ at California Institute of Technology on May 29, 2014

classical cosmic strings, evolving in a ΛCDM cosmological background, these simulations are essentially based on the field theory AH model and the NG model. The latter relies on the assumption that, as the scale of their diameter is much smaller than any cosmological scale, cosmic line-like defects can be studied in the zero-width approximation.

In particular, in NG simulations the time required for the long string component relaxation to the scaling regime in the matter-dominated era can appear decidedly longer than the transient taken to reach scaling in the radiation-dominated era, so that the transition period might last far beyond the end of the decoupling time. Some difference can be found in the NG simulations results related to a different choice of the long component of the network, which can include all loops but those evolving on non-intersecting trajectories (stable loops that cannot rejoin the network; BPOS) or only super-horizon loops. In the latter case, the long string component could reach the scaling regime in a relatively short time, showing little time delay between the change in the expansion law and the response of the network. However, as regards the loop component, its energy density also reaches a scaling evolution but the loop distribution takes more time to reach the scaling regime and the transition period is longer for the smaller loops (BB; RSB).

In AH simulations, the effects of matter–radiation transition are not apparent in the network evolution. The first simulations yield approximately the same value $A_{\rm r} \simeq A_{\rm m} \approx 0.3$ (Bevis et al. 2007), although this result is admittedly a consequence of a simulation size about the minimum required to study a scaling network of strings and recent improved simulations performed by the same authors yield a different result for the scaling parameters in radiation- and matter-dominated eras, with $A_{\rm r} \simeq 0.26$ and $A_{\rm m} \simeq 0.29$ (Bevis et al. 2010).

The reason for differences between simulation results lies mainly in the model at the basis of the simulations. The AH model includes the small-scale physics near the string width, which has a significant role in the string dynamics. While in AH simulations energy from the strings is converted into massive gauge and Higgs radiation through oscillating short-lived loops as well as direct emission, in NG simulations this decay channel is not available and the string length density is significantly higher, with the long strings first converted into small loops and subsequently decaying via gravitational radiation. This additional decay channel in the field theoretic simulations by direct massive radiation may be the primary energy-loss mechanism for long strings and may cause AH strings to scale without gravitational radiation. In the NG scenario, particles are produced only near cusps, which determines much weaker constraints on the production of extremely energetic standard model particles (ultra-high-energy cosmic rays) than in the AH model. On the other hand, in the AH model there are no constraints from gravitational radiation, whereas in the NG case the strongest limits come from millisecond pulsar timing, which depends sensitively on details of the loop distribution and dynamics. The number of loops in the simulation volume is substantially less in field theory simulations than in NG, where a population of non-intersecting loops remaining stable is found, while in AH, where massive radiation is available, loops radiate and shrink. As regards the relevant component for CMB, the long strings, the results yielded by the two types of simulations are quite different in most respects, such as the interstring separation and hence the string density. This latter is significantly lower in the AH than in NG simulations. Similarly, the rms velocities probably due to backreaction from massive radiation are lower in AH than in NG simulations. In fact, AH simulations give $\approx 0.5c$ (Hindmarsh et al. 2009) in both the radiation and matter eras, whereas NG simulations give distinct values in the two cosmological eras, both generally above $0.6c$.

A specific problem related to AH field theory simulations is that computational constraints require the string width to be artificially increased in order to keep it above the simulation resolution. Although this does not significantly affect the CMB power spectra results, a very relevant problem associated with the string width is that the 3D boxes required imply a reduction of the dynamical range. The fact that in AH simulations most of the network energy is emitted through field radiation, until the point that loop production is almost insignificant, has been supposed to be a consequence of low resolution in AH simulations compared to NG ones. On the other hand, the accuracy of the NG simulations with regards to small-scale structure and loop production has also been questioned. In fact, the NG approximation fails close to the string width, i.e. at the cusps and kinks that are expected to form in an intersecting string network. Furthermore, once energy is transferred via intersection events from long strings to small loops, these are assumed to decay into gravitational radiation and are removed from the simulation, since the gravitational waves are not included in any simulation for obvious reasons of complexity connected to backreaction on the string network.

It is worth noting that when simulations involve cosmic superstrings there are none of the aforementioned problems concerning the zero-width approximation. Although cosmic superstrings, as well as conventional cosmic strings, have a tiny but non-zero width, they are theoretically one-dimensional objects. The rich variety of energy loss channels associated with specific properties of such superstrings of cosmic size appears to lead to a rapid approach to the scaling regime for each component of the network.

An alternative approach to field theory cosmic strings consists of using simulations of the NG or AH type and the Unconnected Segment Model (USM). The USM model represents the string network as a stochastic ensemble of unconnected moving segments, of length $Ad_{\rm PH}(t)$ and rms velocity v, which are randomly removed at an appropriate rate so as to find subhorizon decay and the proper string scaling density. The USM model with parameters measured in simulations has been used in the context of CMB anisotropies to reproduce the string power spectra coming from different simulation techniques and derive upper bounds on the string tension parameter (BM). This approach also includes the radiation–matter transition and allows us, in principle, to study the effects of deviations from scaling at the onset of a Λ-dominated phase.

As regards the effects on the CMB of the network evolution during radiation–matter transition, which sets an upper bound to the applicability of equation (14) at redshifts presumably well below $z_{\rm LSS} = 1100$, until about $z \sim 100$, it has been shown (Allen et al. 1996) that the large-scale anisotropies are primarily produced at $z \lesssim 100$. Since the coherence length of the string network grows with time, we expect that anisotropies on small angular scales are seeded at early times and large-angle anisotropies are seeded at late times. Thus, the contribution of cosmic strings in the redshift range $100 < z < 1100$ should only slightly affect the large-angle CMB anisotropy, so that the range of interest (13) in this case can be restricted to $z_0 < z \lesssim 100$. At small angular scales, the relevant contribution to temperature anisotropy induced by cosmic strings comes from the last scattering epoch, where one may expect string signatures in CMB temperature fluctuations to be dominated by their *integrated Sachs–Wolfe* effect from the last scattering surface. It has been shown that at high multipoles the mean angular power spectrum of string-induced CMB temperature anisotropies can be described by a power law slowly decaying as ℓ^{-p}, with

Downloaded from http://mnras.oxfordjournals.org/ at California Institute of Technology on May 29, 2014

$p = 0.889^{+0.001}_{-0.090}$ (Fraisse et al. 2008). This implies that the power spectrum at small angular scales decays much more slowly than the exponential Silk diffusion damping of the CMB primordial anisotropies. Consequently, the cosmic string contribution to the angular power spectrum can be subdominant at low ℓ, while it dominates the primary anisotropies for large values of ℓ. The exponential suppression of the inflationary contribution at high ℓ also means that the string component may dominate for a realistic contribution (i. e. with normalization such that string contribution f_{10} at multipole $\ell = 10$ is 10 per cent of the observed power at this multipole) at $\ell \gtrsim 3500$. The fraction of the total theoretical spectrum due to strings f_ℓ is found to increase (BHKU) from $f_{1500} \approx 0.1$ to $f_{3500} = 0.5$, which suggests that a non-negligible cosmic string contribution to the CMB anisotropies should be searched for at small angular scales, corresponding to $\ell \gtrsim 2000$, as soon as they become accessible. Even though these are the same angular scales for which the *Sunyaev–Zel'dovich* effect begins to make a significant contribution to the temperature power spectrum, this occurs at two observational frequency bands, namely 100 and 150 GHz, whereas the string contribution is at frequencies in observational bands near 220 GHz, where the Sunyaev–Zel'dovich effect is suppressed.

Although the relaxation time for the cosmic string loops to reach a self-similar evolution with respect to the horizon size appears to be larger for smaller loops, the considerable change in scalefactor between the GUT redshift and the last scattering surface might well lead the observable length-scales of the infinite component of the network to be in scaling at decoupling, $z = 1089$. Such scaling long strings may contribute to the CMB anisotropies down to fairly small angles. On the other hand, including the non-scaling loops, field theory numerical simulations show some extra power at very small scales, which suggests that non-scaling structures start to have significant effects at very small scales for $\ell \lesssim 10^4$. As regards the relevant contribution due to the infinite component to the CMB anisotropies at moderately high ℓ, the number of string segments in the corresponding range of redshifts close to $z_{\rm LSS}$, where the network is not expected to have reached the matter era scaling regime, can be estimated as

$$\frac{8\ B^3(z)}{A_{\rm m}^3} < N(z) < \frac{8\ B^3(z)}{A_{\rm r}^3}. \tag{30}$$

Taking into account that it is not known how long the deviation from scaling lasts, $N(z)$ is expected to be closer to the lower or upper bound, depending on how fast the network enters the scaling regime. For cosmic superstrings, the above relation (30) applies to each component of the network; numerical simulations (Pourtsidou et al. 2011) show that the value of $A_{i,j}$ appears generally much closer to $A_{{\rm r},j}$ than it is to $A_{{\rm m},j}$, so that $N_j(z)$ should be near the upper bound.

Let us now consider the deviation from scaling during the matter–dark energy transition, which sets a lower limit at a redshift $z_0 \approx 0.5$ to the applicability of equation (14). The number of cosmic string segments at $z \lesssim 1$ could be extremely small, so that it would become important to understand how deviation from the scaling behaviour around the present cosmological era may affect the network, since an eventual network no longer scaling with matter, exponentially slowed down, could be quite difficult to detect. As previously mentioned, the string velocity plays an important role for detecting signatures in the CMB, since it determines the amplitude of the line-like discontinuities in the CMB temperature. As for the gravitational lensing, there is no such restriction to relativistic velocities required for observations to succeed, but the number of string segments in the range of optical sources could be a very small fraction of the initial number and approaching $z \lesssim 1$ it could become only a small fraction of the expected number in the observable Universe. This can be clearly seen from the values of $N(z)$ for $z \in (0.5, 7]$ presented in Table 2 for field theory cosmic strings and in Tables 3 and 4 for string theory cosmic superstrings.

Thus, assuming that the most distant objects we are able to observe by optical methods are located at a redshift $z = 7$, the probability of observing segments of the strings crossing the effective observable Universe in the optical range is proportional to the volume of the optical sphere, having radius $d(z = 7) = B(z = 7)d_{\rm PH}$. In horizon units, then, in a ΛCDM cosmological background, we have $p \sim B^3(7) = 0.22$ and the present angular size of a string having its centre at this redshift is $\sim 100^\circ$ (Sazhina et al. 2008), whereas the angular size of a segment of length $L(z = 7)$ eventually observed is about 7°. For smaller values of redshift, the number of string segments inside the corresponding sphere becomes increasingly smaller and the angular size of the string with a centre at that redshift becomes larger. For instance, at redshift $z = 2$ the probability is reduced to $p \sim B^3(2) = 0.05$ and the current angular size of the string is around 134°, while for a segment $L(z = 2)$ the angular size we should observe is about 20°. Below $z \lesssim 1$, the number of string segments inside the sphere of radius $d(z \lesssim 1)$ is expected to be so small as to render detection by optical methods in this range a challenging problem, unless the deviation from scaling at transition to the dark energy era is such that the decrease in reconnection events, the effect of which is to increase the density of strings and the time needed to reach equilibrium, may somewhat compensate for the eventual dilution by exponential expansion, maintaining the number of strings at a detectable level.

Regarding the dark energy variants of the standard cosmology, a different choice of the equation-of-state parameter implies increasing or decreasing distances and hence the volumes defined through such distances. These volume effects are due to a different expansion rate: phantom models always have a larger volume than the ΛCDM model, since the expansion rate is larger, while quintessence models have a smaller volume than the ΛCDM model, the expansion rate being lower. As a consequence, one can only find an increased or decreased number of string segments, since the characteristic length-scale of the network is unaltered. The number of string segments for $w \in \{-1.5, -1, -0.5\}$ is presented in Table 2.

As we can see from Fig. 1, $N(z)$ is strongly dependent on w. The graph refers to NG strings but the trend is the same, decreased by a factor of about 4, for AH strings. A comparison of the results obtained in the two ranges of the optical sources, up to $z = 7$, and radio surveys, covering all z up to last scattering time, shows that the distribution of string segments could be sufficient to leave detectable signals through gravitational lensing and in the CMB radiation for NG strings, whatever the expansion rate.

The density of step-like temperature discontinuities in the CMB radiation (KS effect) produced by cosmic strings crossing the last scattering surface is determined by the number density of string segments in that volume. On the other hand, deviations from the ideal condition on the string orientation $\hat{k} \cdot (\hat{\beta}_{\rm s} \times \hat{s}) = 1$ (where $\hat{k}$, $\hat{s}$ and $\hat{\beta}_{\rm s}$ are respectively the unit vectors along the line of sight, the string and its direction of motion) lead to

$$\frac{\delta T}{T} = \Delta\gamma_{\rm s}\beta_{\rm s} \tag{31}$$

(where $\gamma_{\rm s}$ is the Lorentz factor for the string segment) and imply that not all of the string segments distributed on the last scattering surface may leave detectable signatures in the CMB radiation; in the most favourable case, the amplitude $\delta T/T$ of the temperature

Downloaded from http://mnras.oxfordjournals.org/ at California Institute of Technology on May 29, 2014

Table 5. $N^{\rm obs}(z, \theta < \pi/2)$ is the probability of observing string segments that form an angle θ with respect to the line of sight for sources distributed at $z_{\rm s} \in [1, 2]$ for different models. Δz is the range of string-segment redshifts that define the spherical shells considered for the lensing-angle observations. $\theta < \pi/2 : \delta\phi = 0.05$ arcsec refers to the largest and smallest deviations from the ideal case such that the lensing angle is detectable for $z_{\rm s} \in [1, 2]$ when an angular resolution 0.05 arcsec can be reached. $\delta\phi\,(\theta = \pi/2)$ refers to the maximum value taken by the lensing angle in the ideal case, corresponding to the largest distance string–source for all sources in the interval $z_{\rm s}$.

Model	$N^{\rm obs}(z, \theta < \pi/2)$	Δz	$\theta < \pi/2 : \delta\phi = 0.05$ arcsec	$\delta\phi\,(\theta = \pi/2)$ arcsec
P (NG)	81 per cent $z_{\rm s} \in [1, 2]$	$z \in [0.6, 1)$	$7\pi/180$–$17\pi/36$	0.25–0.42
	64 per cent $\forall z_{\rm s} \in [1, 2]$	$\tilde{z} \in [0.6, 0.91]$		
	35 per cent	$z \in [1, 2)$	$\pi/15$–$7\pi/15$	0.9–0.26
	$z_{\rm s} \in (1, 2]$	$z^{\rm obs} \in [1, 1.76]$		
P (AH)	91 per cent $z_{\rm s} \in [1, 2]$	$z \in [0.6, 1)$	$\pi/45$–$11\pi/36$	0.55–0.93
	81 per cent $\forall z_{\rm s} \in [1, 2]$	$\tilde{z} \in [0.6, 0.95]$		
	60 per cent	$z \in [1, 2)$	$\pi/36$–$17\pi/45$	0.11–0.58
	$z_{\rm s} \in (1, 2]$	$z^{\rm obs} \in [1, 1.88]$		
Λ (NG)	80 per cent $z_{\rm s} \in [1, 2]$	$z \in [0.6, 1)$	$7\pi/180$–$22\pi/45$	0.24–0.42
	63 per cent $\forall z_{\rm s} \in [1, 2]$	$\tilde{z} \in [0.6, 0.91]$		
	36 per cent	$z \in [1, 2)$	$\pi/15$–$22\pi/45$	0.09–0.27
	$z_{\rm s} \in (1, 2]$	$z^{\rm obs} \in [1, 1.77]$		
Λ (AH)	91 per cent $z_{\rm s} \in [1, 2]$	$z \in [0.6, 1)$	$\pi/45$–$14\pi/45$	0.54–0.93
	81 per cent $\forall z_{\rm s} \in [1, 2]$	$\tilde{z} \in [0.6, 0.95]$		
	61 per cent	$z \in [1, 2)$	$\pi/36$–$7\pi/15$	0.11–0.59
	$z_{\rm s} \in (1, 2]$	$z^{\rm obs} \in [1, 1.89]$		
Q (NG)	79 per cent $z_{\rm s} \in [1, 2]$	$z \in [0.6, 1)$	$2\pi/45$–$4\pi/9$	0.23–0.41
	58 per cent $\forall z_{\rm s} \in [1, 2]$	$\tilde{z} \in [0.6, 0.9]$		
	35 per cent	$z \in [1, 2)$	$\pi/15$–$4\pi/9$	0.085–0.25
	$z_{\rm s} \in (1, 2]$	$z^{\rm obs} \in [1, 1.76]$		
Q (AH)	90 per cent $z_{\rm s} \in [1, 2]$	$z \in [0.6, 1)$	$\pi/45$–$13\pi/36$	0.51–0.9
	80 per cent $\forall z_{\rm s} \in [1, 2]$	$\tilde{z} \in [0.6, 0.95]$		
	60 per cent	$z \in [1, 2)$	$\pi/30$–$7\pi/15$	0.1–0.57
	$z_{\rm s} \in (1, 2]$	$z^{\rm obs} \in [1, 1.89]$		
D strings	93 per cent $z_{\rm s} \in [1, 2]$	$z \in [0.6, 1)$	$\pi/60$–$4\pi/15$	0.77–1.3
$g_{\rm s} = 0.04$	85 per cent $\forall z_{\rm s} \in [1, 2]$	$\tilde{z} \in [0.6, 0.96]$		
	70 per cent	$z \in [1, 2)$	$\pi/45$–$2\pi/5$	0.15–0.84
	$z_{\rm s} \in (1, 2]$	$z^{\rm obs} \in [1, 1.92]$		

fluctuations would be an order of magnitude lower than the adiabatic fluctuations ($\sim 10^{-5}$). In fact, two positive factors less than 1 appear at the right hand side of equation (31) when the unit vectors $\hat{k}$, $\hat{s}$ and $\hat{\beta}_s$ are not mutually perpendicular. This could render very difficult to have signals that are statistically significant and unambiguously identifiable as sourced by such cosmic strings, especially if the underlying cosmological model is a quintessence model and the string evolution is described by the AH model.

Regarding cosmic superstrings, the small value of the deficit angle that is found for the F component in the limit $g_{\rm s} \sim 10^{-2}$, $\Delta \sim 0.09$ arcsec leads to temperature jumps in the CMB radiation that are no longer appreciable, so that the presence of a large number of F strings does not conflict with observations. As for the D component of the network, although the temperature discontinuities span the wide volume of the Universe enclosed by the last scattering surface, the number of D-string segments up to $z = 1100$ remains quite small and the number of bound states is expected to be still smaller. Consequently, the probability of observing peculiar temperature patterns due to Y junctions appears to be very low, especially when observations are performed with ground-based telescopes having a limited field of view covering only part of the sky. For similar reasons, in the range of z of interest for gravitational lensing effects, as we shall see in Section 4.2, the observation might be quite challenging, especially if cosmic strings are not perpendicular to the line of sight.

4.2 On the observation of gravitational lensing by cosmic strings

The difference between the two classical models describing the evolution of cosmic strings is quite significant and is almost of the same level for the different cosmological models describing the background in which they evolve. Therefore, for the considerations that follow, for definiteness as regards field theory cosmic strings we refer mainly to the ΛCDM cosmology, but extension to the above-mentioned variants and to superstring theory cosmic strings is discussed as well and is summarized in Table 5.

Although the constraint on the string tension parameter set by gravitational lensing is $G\mu/c^2 < 3 \times 10^{-7}$ (Christiansen et al. 2011), we will take into account the stricter constraint coming from the CMB power spectrum and try to obtain some further insight into the probability of observing cosmic strings through gravitational lensing events. We will consider ideal strings, i.e. cosmic strings approximately straight on the length L of the step of the random walks that they form.

The Atacama Cosmology Telescope (Dunkley et al. 2011) and *Planck* data [Ade et al. (Planck Collaboration) 2013b] provide, for NG strings, respectively $G\mu/c^2 < 1.6 \times 10^{-7}$ and $G\mu/c^2 < 1.5 \times 10^{-7}$. For AH cosmic string networks, the limit $G\mu/c^2 < 3.2 \times 10^{-7}$ is found in the *Planck* data. According to the above stringent constraints, let us consider what happens for static strings when

Downloaded from http://mnras.oxfordjournals.org/ at California Institute of Technology on May 29, 2014

the ideal condition of perpendicularity between string orientation and the line of sight is dropped, i.e. when $\gamma_s(1+\hat{k}\cdot\boldsymbol{\beta}_s)|\hat{k}\times\hat{s}| = \sin\theta$ and the angular separation between the lensed images is given by

$$\delta\phi = \Delta\frac{D_{ls}}{D_{os}}\sin\theta, \qquad \theta\in[0,\pi]\,. \tag{32}$$

Since the lensing angle depends on Δ as well as on the ratio between the angular diameter distances from source to string (lens), D_{ls}, and from source to observer, D_{os}, and on the angle θ between the string direction and the line of sight, not all strings contained in the sphere of optical sources can be observed through their gravitational lensing effects. For a straight string segment lying at z close to the upper limit of the optical range, the corresponding lensing angle would be on the border of observability ($\lesssim$0.05 arcsec), since $D_{ls} \ll D_{os}$, even in the ideal case $\sin\theta = 1$, although $N(z)$ is still quite large for NG strings compared with the AH case. For instance, in a ΛCDM cosmology, we have $N(z) \sim 250$ for NG strings and $N(z) \sim 50$ for AH strings. For the most distant sources at $z_s \sim 6$–7, therefore, the string–lens is required to be at $z \lesssim 5$ in order to yield observable effects. For non-ideal strings, an additional factor less than unity for $\theta \neq \pi/2$ restricts the strings with greater probability of being observed to those located at redshifts around $z \lesssim 2$ (where, on average, the number of string segments is expected to be <55 for the NG model and <12 for the AH model). This implies a cut for the lens location on the highest values of z in the optical sources range at redshifts where the expected number of string segments, at least in the NG case, is sufficiently large. Setting a lower bound on the possible redshifts at which one can reasonably expect to find more than one string across the observed sky at the redshift of the transition matter–dark energy results in a further reduction of the probability of observing gravitational lensing events for the large number of sources (quasars and galaxies) distributed around $z_s \sim 2$, as well as for the most distant and rare sources.

If we consider that most observed quasars and galaxies are distributed at redshifts $1 \lesssim z_s \lesssim 2$ (Conselice 2004; Stott et al. 2013 and references therein), the range of redshifts at which the probability of observing cosmic strings by their gravitational lensing effects is greatest will be $0.6 \leq z < 1$. For a source at $z_s \in [1, 2]$ and a segment of string at a redshift $z \in [0.6, 1)$, up to values of z having a proximity to the upper limit that is model-dependent, the corresponding lensing angle is in principle always sufficiently large for ideal strings to produce two distinguishable images of the source when this is a quasar. As regards galaxies, only the points interior to the strip defined by the deficit angle will appear duplicated the other side of the string. The outer points will be cut away, resulting in visible sharp edges in the isophotes of the source images (Sazhin et al. 2007). However, for $z < 1$, N(z) is less than 15 for NG strings and no more than 3 for AH strings in a ΛCDM cosmological background. As for quintessence and phantom field models, the lower and higher number of segments at such z is significant only for NG models.

Even choosing a value of the NG string tension parameter very close to the upper bound coming from the *Planck* data, the deficit angle Δ will be quite small, being no more than 0.77 arcsec. Consequently, for cosmic strings with orientations that do not match the ideal condition, though they are located close to the lower limit of the matter-dominated era, for some values of θ the corresponding lensing angle can be too small to be observable. Let us consider, for instance, randomly oriented static strings located at redshifts $0.6 \leq z < 1$, which could be gravitational lenses for any sources in the above-mentioned redshift range. Outside a certain interval of values of θ, $\delta\phi$ becomes smaller than the angular resolution of current space-based telescopes (ranging from 0.1 arcsec to 0.05 arcsec). For any source considered, this interval is essentially dependent on the string redshift. Thus, in order to have an idea of the number of potentially observable string segments for any value of that range of z and for any value of the source redshift $z_s \in [1, 2]$, we have to calculate the probability of observing a segment of cosmic string, in a given volume, that forms with the line of sight an angle θ contained in the corresponding interval for each interval separately. By adding the results, we find that the total number of segments of a static straight string which can produce observable gravitational lensing effects for sources located at $z_s \in [1, 2]$, depending on the angular resolution of the telescope, for all the considered cosmological background is reduced by an amount that ranges from about one-fifth (for an angular resolution of 0.05 arcsec) to half (for an angular resolution of 0.1 arcsec) of the expected number of string segments at $z \in [0.6, 1)$. For AH cosmic strings, the constraint on the tension parameter set by the *Planck* data is less strong and consequently the deficit angle can reach 1.7 arcsec, meaning that, although for $z \in [0.6, 1)$ for any cosmological model we always have $N(z) < 4$, almost all of these string segments, however far from the ideal condition in many cases, can give rise to detectable lensing angles.

In Table 5, the second column, N^{obs}, represents the number of string segments that can produce a detectable $\delta\phi$ with respect to the number of segments expected in the spherical shell under consideration. In particular, the results relative to string segments outside and inside the source region are shown separately in the subsequent lines of each row 'model' of the table. In the range of the string redshift outside the one chosen for sources, all the string segments in the shell determined by $z \in [0.6, 0.99]$ will give detectable $\delta\phi$ in the case of ideal strings. This number is reduced by an amount dependent primarily on the model describing cosmic strings and to a lesser extent on the cosmological model. The values of the tension parameter chosen for calculation are 1.4×10^{-7} and 3.1×10^{-7} for classical NG and AH strings, respectively, and 4.4×10^{-7} for the string theory D strings.

Noticing that N^{obs} does not provide the probability of observing the effects of gravitational lensing by cosmic strings, which cannot be taken into account irrespective of the distribution of sources, but only the probability of having $\delta\phi$ sufficiently large to be detected, the range of values of redshift with which a higher probability of observation may actually be associated is that for which $\delta\phi$ is detectable for any z_s. The corresponding number of segments that produce such $\delta\phi$ will be somewhat lower than that given in the first line of the table, relative to the interval [0.6, 1), and regards string segments having z that varies in a model-dependent narrower range, $\tilde{z}$. As we can see in the second line of the corresponding row 'model' of Table 5, about 80 per cent of the segments that can yield observable lensing angles for the NG models and about 90 per cent for the AH models are further reduced, on average, to less than 65 per cent and around 80 per cent, respectively, if we consider string–source distances such that the segments can be observed as gravitational lenses for all sources in the redshift range $z_s \in [1, 2]$. Of course, even for an ideal orientation of strings there will be a reduction in the number of observable objects, due to a lens–source distance too close. The range of z for the segments of string, $\tilde{z}$, that can be observed by means of lensing effects for all z_s is almost the same for both ideal and non-ideal cases, but the number of objects potentially observable is quite different. For example, for NG strings in a ΛCDM cosmological background, this difference amounts to ~77 per cent for strings with ideal orientation compared

Downloaded from http://mnras.oxfordjournals.org/ at California Institute of Technology on May 29, 2014

with the ∼63 per cent reported in the table for randomly oriented strings.

In Table 5, the maximum value of $\delta\phi$ when $\theta = \pi/2$ is also shown for sources between $z_s = 1$ and $z_s = 2$. The lowest value of $\delta\phi$, assumed at the smallest distances string–source, is taken to be the angular resolution 0.05 arcsec. How small this distance can be depends more consistently on the cosmic string model than the cosmological model, as well as the largest value that $\delta\phi$ can assume, in correspondence to the largest distance lens–source also reported in the table. This last column shows how the two quantities $r = D_{ls}/D_{os}$ and Δ in equation (32), related respectively to the cosmological model and the cosmic string model, affect the value of $\delta\phi$ and indicates the maximum values that can be reached in the best possible situation of mutual distances string–source–observer. A large range of the allowed deviation from the ideal case, given by the first number of the θ column, is associated with this 'best situation'. For instance, for NG strings in a ΛCDM cosmology, θ can vary from 7°–90°, with detectable values of $\delta\phi$ ranging from 0.05 arcsec to the interval of values given in the last column. In the fourth column, the values of the maximum and minimum deviation θ such that the lensing angle is observable, as functions of the distance string–source, show that when D_{ls} becomes very small we can have $\delta\phi$ observable only for θ values very close to 90°, i.e. only for strings nearly perpendicular to the line of sight. For instance, for a NG model in a ΛCDM cosmological background, $\delta\phi$ is detectable for z of the lens very close to $z_s = 1$, $z = 0.91$, only if $\theta \geq 88°$, i.e. for strings with almost-ideal orientation, while for P models a greater deviation from the ideal condition is possible and the same distance in a Q model does not provide a detectable $\delta\phi$ even in the ideal case. A very small allowed deviation from the perpendicularity between the string and the line of sight is confined to the case of very small lens–source distances. In the majority of cases, significant deviations from the ideal case can be considered, meaning that realistic cosmic strings may have detectable gravitational lensing effects to an extent that is not too far from the upper bound exhibited in Table 5. Regarding the AH strings, for any cosmological model very close distances lens–source, as well as quite large deviations from the ideal case, may produce a detectable $\delta\phi$. This is also true for D strings. However, whatever the considered model and distance lens–source, the range of θ for which $\delta\phi$ is detectable never includes all values of θ. The largest interval is obtained for D strings: $\delta\phi \geq 0.05$ arcsec for $\theta \geq 3°$.

When the lens is at a redshift $1 \leq z < 2$, within the volume considered for the sources, as z increases, the ratio between the angular distances D_{ls} and D_{os} decreases so that even small deviations from the ideal case can yield undetectable lensing angles. For NG strings, $\delta\phi$ is no longer detectable for $z \sim 1.8$ even for cosmic strings with ideal orientation and assuming an angular resolution of 0.05 arcsec. Of all the string segments contained in the spherical shell determined by $z \in [1, 2)$, only a small fraction may have a $\delta\phi$ potentially observable for sources at $z_s \in (1, 2]$. For the AH models, although the expected number of string segments at $z \in [1, 2)$ ranges from 2–4 to 6–15, since the deficit angle is large enough, a large number of them (∼60 per cent) can produce a $\delta\phi$ detectable up to $z \sim 1.9$, for sources at $z_s \in (1, 2]$ for some values of θ of randomly oriented strings. In Table 5, z^{obs} provides the range of redshifts for string segments within the region of sources to have detectable $\delta\phi$ when some deviation from the ideal condition is taken into account.

As can be seen in the above-mentioned table, ΛCDM and P models show very little difference in the percentage of objects that can produce detectable lensing effects. In this interval of string redshift, apart from the number of possible lenses, which certainly is not very high, the reduction of the number of possible sources as z increases is also crucial.

The small increase in N^{obs} resulting in the case of a ΛCDM model compared with a P model case, apparently in contrast with what happens in the range of z of the string–lens outside the region where the sources are located, is explained by the different trend of the ratio $r = D_{ls}/D_{os}$, which, for strings at $z \in [1, 2)$ and for growing values of the redshift of the string approaching the source close to the upper bound of the considered region, reverses its behaviour by passing from $r_P > r_\Lambda$ to $r_\Lambda > r_P$, while this never occurs for strings at $z \in [0.6, 1)$. For quintessence NG and AH models, since it is always $r_Q < r_\Lambda$ and it is $r_Q > r_P$ only for the lens location close to the source at z_s near the upper limit, N_{obs} in this range of string redshift becomes comparable to that obtained for NG and AH phantom field models.

N^{obs} shows some difference among cosmic string models and little difference among cosmological models as regards the reduction due to deviations from the ideal case. This was expected, since the different value of Δ affect the results more than the difference in the ratio r. As a consequence, the number of expected segments being different for different cosmological models, we will end up with a different number of objects observable through gravitational lensing effects. Evidently, the worst situation is given by the Q models. In this respect, it is worth mentioning that *Planck* observations show that CMB data are compatible with a cosmological constant, as assumed in the ΛCDM model, whereas additional SNLS SNe data favour the phantom domain $w < -1$ [Ade et al. (Planck Collaboration) 2013a, and references therein].

It is worth pointing out that, according to the representation suggested by the scaling solution, a network of random walk strings can be approximated by a collection of straight string segments, of length given by the step of the random walk, fairly uniformly distributed. The string segments have random orientation and move with randomly directed velocities. Since strings are relativistic, at each Hubble time a different distribution of cosmic string segments affects the photons propagating freely after the last scattering or emitted at later times by galaxies. We consider the centres of string segments located at different redshift to estimate the approximate number of string segments inside our backward light cone. At any time t_* before t_0, considering the set of all events in the past light cone of the observer at t_0 that occur at time t_*, the result would be a sphere centred on the present observer with a radius given by the distance travelled by photons from that time to today. Any point on or inside the sphere could send a signal moving at the speed of light or slower that would have time to reach the observer at t_0, while points outside the sphere at that moment would not be able to have any causal contact with the present observer. Since we wish to detect cosmic strings not through direct emission but by means of photon worldlines interconnected with the string worldsheets, in order to find the effective number of segments that produce deflection and frequency shift of photons, the light-cone projection of the string segments needs to be considered (see e.g. Hindmarsh 1994).

An exhaustive treatment on the topic involving survey fields, the distribution of sources at different redshifts and their brightnesses, the string velocity and effects due to the 'wiggliness' is beyond the scope of this article. Here we only mean to point out the extent to which the underlying models, for either the cosmological background or cosmic strings, can make the difference between having observable effects or not. To show this, we focused on the most favourable redshift range of sources, i.e. around the star

Downloaded from http://mnras.oxfordjournals.org/ at California Institute of Technology on May 29, 2014

formation peak where the observed objects are more numerous and brighter.

The outcome of the above discussion is in large part a consequence of the small value of the deficit angle Δ, as we have shown. Thus, when we apply the same considerations to cosmic superstrings we find significant differences due to the fact that, for a small value of the string coupling constant ($g_s \sim 10^{-2}$), while the D and FD components of the network have tensions comparable to those of ordinary cosmic strings, the F component is expected to have smaller tension, $G\mu_F/c^2 \leq 1.8 \times 10^{-8}$. This leads to very small values of the lensing angle, $\delta\phi < 0.05$ arcsec, which prevents any optical identification even in the ideal case of string segments perpendicular to the line of sight. As a consequence, although a small value of the string coupling constant yields an exceedingly large number of string segments ($\sim 10^3$) for the F component even at small redshifts (down to the value $z \sim 0.6$) against the small number found for ordinary cosmic strings, models supporting a small value of the string coupling constant cannot be ruled out on the grounds of the predicted large number of the F component, as long as the range of small values of tension involved is still unexplored by means of current technology. We will not dwell on the case $g_s = 0.9$, considering the relative results only by way of comparison with the interesting opposite case of small values of the string coupling constant. In fact, models with a small g_s, which ensure a compactification scale exceeding or equal to the four-dimensional GUT scale and lead to a low-energy supergravity, also allow us to work in a perturbative regime in a way consistent with the underlying theory. A small value of the deficit angle such as the one obtained for the F component in the limit $g_s \sim 10^{-2}$, $\Delta \sim 0.09$ arcsec, leads to undetectable lensing angles. On the other hand, as regards the D component of the network, since it is $G\mu_D/c^2 \leq 4.5 \times 10^{-7}$ the deficit angle approaches the value 2.3 arcsec, thus leading to detectable gravitational lensing effects for about 80 per cent of the randomly oriented segments of D strings in the entire volume considered. Cosmic superstrings can produce detectable $\delta\phi$ up to very short string–source distances and with a greater allowed deviation from the ideal condition for observations.

Although $\mu_{FD} \simeq \mu_D$, the very small number of FD strings leads to the conclusion that if for D strings, as well as for traditional strings, gravitational lensing is expected to be a very rare event, this is even more true in the case of the Y junctions that may form from FD bound states.

ACKNOWLEDGEMENTS

The authors thank Cosimo Stornaiolo for helpful discussions. The research was financially supported by the grant RFFI 10-02-00961a. The work was carried out as part of the project No. 14.740.11.0085 of the Ministry of Education. RC acknowledges partial financial support by the NASA–Jet Propulsion Laboratory and the kind hospitality of the California Institute of Technology, where this work was partly carried out. Furthermore the authors acknowledge the use of the Legacy Archive for Microwave Background Data Analysis (LAMBDA), part of the High Energy Astrophysics Science Archive Center (HEASARC). HEASARC/LAMBDA is a service of the Astrophysics Science Division at the NASA Goddard Space Flight Center.

REFERENCES

Achucarro A., de Putter R., 2006, Phys. Rev. D, 74, 121701
Ade P. A. R. et al. (Planck Collaboration), 2013a, preprint (arXiv:1303.5076)
Ade P. A. R. et al. (Planck Collaboration), 2013b, preprint (arXiv:1303.5089)
Albrecht A., Battye R. A., Robinson J., 1998, Phys. Rev. D, 59, 023508
Allen B., Shellard E. P. S., 1990, Phys. Rev. Lett., 64, 119 (ASb)
Allen B., Caldwell R. R., Shellard E. P. S., Stebbins A., Veeraraghavan S., 1996, Phys. Rev. Lett., 77, 3061
Antoniadis I., Arkani-Hamed N., Dimopoulos S., Dvali G., 1998, Phys. Lett. B, 436, 257
Arkani-Hamed N., Dimopoulos S., Dvali G., 1998, Phys. Lett. B, 429, 263
Avgoustidis A., Shellard E. P. S., 2005, Phys. Rev. D, 73, 041301
Battye R., Moss A., 2010, Phys. Rev. D, 82, 023521 (BM)
Battye R. A., Robinson J., Albrecht A., 1998, Phys. Rev. Lett., 80, 4847
Bennett D. P., Bouchet F. R., 1990, Phys. Rev. D, 41, 2408 (BB)
Bevis N., Hindmarsh M., Kunz M., Urrestilla J., 2007, Phys. Rev. D, 76, 043005
Bevis N., Hindmarsh M., Kunz M., Urrestilla J., 2010, Phys. Rev. D, 82, 065004 (BHKU)
Blanco-Pillado J. J., Olum K. D., Shlaer B., 2011, Phys. Rev. D, 83, 083514 (BPOS)
Bolotin Y. L., Lemets O. A., Yerokhin D. A., 2012, Phys. Usp., 55, 876
Caldwell R. R., 2002, Phys. Lett. B, 545, 23
Christiansen J. L., Albin E., Fletcher T., Goldman J., Teng I. P. W., Foley M., Smoot G. F., 2011, Phys. Rev. D, 83, 122004
Conselice C. J., 2004, preprint (arXiv:astro-ph/0407463)
Copeland E. J., Myers R. C., Polchinski J., 2004, J. High Energy Phys., 0406, 013
Copeland E. J., Sami M., Tsujikawa S., 2006, Int. J. Mod. Phys. D, 15, 1753
Dunkley J. et al., 2011, ApJ, 739, 52
Durrer R., 1999, New Astron. Rev., 43, 111
Firouzjahi H., 2008, Phys. Rev. D, 77, 023532
Fraisse A. A., Ringeval C., Spergel D. N., Bouchet F. R., 2008, Phys. Rev. D, 78, 043535
Frieman J., Turner M., Huterer D., 2008, ARA&A, 46, 385
Henry Tye S. H., Wasserman I., Wyman M., 2005, Phys. Rev. D, 71, 103508 [Erratum; 71, 129906 (2005)]
Hindmarsh M., 1994, ApJ, 431, 534
Hindmarsh M. B., Kibble T. W. B., 1994, Rept. Prog. Phys., 58, 477
Hindmarsh M., Stuckey S., Bevis N., 2009, Phys. Rev. D, 79, 123504
Jackson M. G., Jones N. T., Polchinski J., 2005, J. High Energy Phys., 0510, 013
Jones N., Stoica H., Henry Tye S. H., 2003, Phys. Lett. B, 563, 6
Kachru S., Kallosh R., Linde A., Maldacena J., McAllister L., Trivedi S. P., 2003, J. Cosmol. Astro-Particle Phys., 0310, 013
Kaiser N., Stebbins A., 1984, Nature, 310, 391
Kibble T. W. B., 1976, J. Phys. A, 9, 1387
Martins C. J. A. P., Shellard E. P. S., 2006, Phys. Rev. D, 73, 043515 (MS)
Pourtsidou A., Avgoustidis A., Copeland E. J., Pogosian L., Steer D. A., 2011, Phys. Rev. D, 83, 063525
Riess A. G. et al., 2004, ApJ, 607, 665
Ringeval C., Sakellariadou M., Bouchet F. R., 2007, J. Cosmol. Astro-Part. Phys., 0702, 023 (RSB)
Sazhin M. V., Khovanskaya O. S., Capaccioli M., Longo G., Paolillo M., Covone G., Grogin N. A., Schreier E. J., 2007, MNRAS, 376, 1731
Sazhin M. V., Sazhina O. S., Capaccioli M., Longo G., Paolillo M., Riccio G., 2010, Open Astron. J., 3, 200
Sazhina O. S., Sazhin M. V., Sementsov V. N., Capaccioli M., Longo G., Riccio G., D'Angelo G., 2008, preprint (arXiv:0809.0992)
Shellard E. P. S., Allen B., 1990, in Gibbons G. W., Hawking S. W., Vachaspati T., eds, Formation and Evolution of Cosmic Strings. Cambridge Univ. Press, Cambridge (ASa)
Stott J. P. et al., 2013, MNRAS, 430, 1158
Vachaspati T., 2001, preprint (arXiv: hep-ph/0101270)
Vilenkin A., Shellard E. P. S., 1995, Cosmic Strings and other Topological Defects. Cambridge Univ. Press, Cambridge

This paper has been typeset from a TEX/LATEX file prepared by the author.

Downloaded from http://mnras.oxfordjournals.org/ at California Institute of Technology on May 29, 2014